

Supplementary Information

for

“Elucidation of Protein-Ligand Interactions by Multiple
Trajectory Analysis Methods”

Nian Wu^{1, #, *}, Ruotian Zhang^{1, #}, Xingang Peng¹, Lincan Fang², Kai Chen³, Joakim S.
Jestilä²

**1 Institute for Interdisciplinary Information Sciences, Tsinghua University,
Beijing, China.**

2 Applied Physics, Aalto University, Espoo, Finland.

3 Institute of Catalysis, Zhejiang University, Hangzhou, China.

These authors contributed equally.

*** All correspondence should be addressed to wunianwhu@gmail.com.**

Table S1: Information of the selected 100 ligand-protein complexes

	pdbid	uniprot	measure	affinity	unit	affinity(-logKd)
0	4xtx	I6YFP0	Kd	0.027	nM	10.57
1	4rfm	Q08881	Ki	0.09	nM	10.05
2	4xtz	I6YFP0	Kd	0.153	nM	9.82
3	3lxk	P52333	Kd	0.16	nM	9.8
4	4cd0	Q9UM73	Ki	0.2	nM	9.7
5	5anu	P36639	Kd	0.4	nM	9.4
6	4crf	P03951	Ki	0.5	nM	9.3
7	3vhd	P07900	Kd	0.52	nM	9.28
8	2xab	P07900	Kd	0.54	nM	9.27
9	4clj	Q9UM73	Ki	0.7	nM	9.15
10	3d91	P00797	Ki	0.7	nM	9.15
11	2xjx	P07900	Kd	0.71	nM	9.15
12	3gnw	O92972	Kd	0.79	nM	9.1
13	5lwm	P52333	Kd	1.34	nM	8.87
14	5cas	P00533	Ki	1.4	nM	8.85
15	5uoo	O60885	Ki	1.4	nM	8.85
16	5e2p	P03951	Ki	1.6	nM	8.8
17	4x6o	P03951	Ki	1.9	nM	8.72
18	5mpk	Q92793	Kd	3	nM	8.52
19	4y8x	P03951	Ki	3.7	nM	8.43
20	3zxz	P08581	Ki	4	nM	8.4
21	5fck	P00746	Kd	6	nM	8.22

22	4pop	A2RI47	Kd	7.44	nM	8.13
23	3gvu	P42684	Kd	10	nM	8
24	1fkg	P62942	Ki	10	nM	8
25	3r4p	P07900	Ki	11	nM	7.96
26	5i1q	P21675	Kd	12	nM	7.92
27	4w9p	Q13451	Ki	16	nM	7.8
28	5ueu	O60885	Ki	16.7	nM	7.78
29	4w9o	Q13451	Ki	17	nM	7.77
30	3tzm	P36897	Ki	17	nM	7.77
31	1lee	P46925	Ki	18	nM	7.74
32	4auj	A2IC68	Kd	18.3	nM	7.74
33	3rlr	P07900	Ki	30	nM	7.52
34	5nlk	Q92793	Kd	35	nM	7.46
35	1b5j	P06202	Kd	37	nM	7.43
36	4kn0	P14207	Kd	40	nM	7.4
37	2j7e	Q08638	Kd	48	nM	7.32
38	6ckr	O60885	Kd	50	nM	7.3
39	4xit	P07900	Ki	54	nM	7.27
40	1q7a	P59071	Kd	64	nM	7.19
41	2i6b	Q5VXR3	Kd	68	nM	7.17
42	3rlp	P07900	Kd	84	nM	7.08
43	4xiq	P07900	Ki	86	nM	7.07
44	4fcq	P07900	Kd	101	nM	7
45	4att	A2IC68	Kd	104.6	nM	6.98

46	3pn1	P43813	Ki	110	nM	6.96
47	5ie1	P56817	Kd	140	nM	6.85
48	1fhd	P07986	Ki	150	nM	6.82
49	4nue	O60885	Ki	150	nM	6.82
50	6fo5	O60885	Kd	190	nM	6.72
51	2fqw	P29724	Kd	210	nM	6.68
52	5op5	O14757	Ki	216	nM	6.67
53	1pxp	P24941	Ki	220	nM	6.66
54	4xip	P07900	Ki	235	nM	6.63
55	4btk	Q5TCY1	Kd	240	nM	6.62
56	3sr4	Q8TEK3	Ki	290	nM	6.54
57	2xjj	P07900	Kd	310	nM	6.51
58	5uc4	P08238	Kd	350	nM	6.46
59	1fh9	P07986	Ki	370	nM	6.43
60	2w9h	P0A017	Kd	430	nM	6.37
61	5ant	P36639	Kd	440	nM	6.36
62	3k5v	P00520	Kd	500	nM	6.3
63	5lz7	Q13093	Kd	530	nM	6.28
64	4bqg	Q2VPJ6	Kd	600	nM	6.22
65	1sqt	P00749	Ki	630	nM	6.2
66	5kax	Q8KFZ1	Kd	780	nM	6.11
67	5fso	P36639	Kd	810	nM	6.09
68	5h9r	P17931	Kd	840	nM	6.08
69	5d3l	O60885	Kd	880	nM	6.06

70	4nuc	O60885	Ki	910	nM	6.04
71	4km0	P0A546	Kd	910	nM	6.04
72	2xht	P07900	Kd	1100	nM	5.96
73	5eng	Q92793	Kd	1400	nM	5.85
74	4km2	P0A546	Kd	1430	nM	5.84
75	5tb6	Q92793	Kd	1530	nM	5.82
76	6ey8	P07900	Kd	1550	nM	5.81
77	6eog	P17931	Kd	1600	nM	5.8
78	5fsn	P36639	Kd	1700	nM	5.77
79	5mwh	P55201	Kd	1800	nM	5.74
80	5n18	Q5A4W8	Kd	2100	nM	5.68
81	2ojg	P28482	Ki	2300	nM	5.64
82	2uy5	P29029	Ki	3200	nM	5.49
83	4jfm	Q13451	Kd	3300	nM	5.48
84	1b46	P06202	Kd	5200	nM	5.28
85	5o5a	P55201	Kd	17000	nM	4.77
86	5lne	Q1RBS0	Kd	17430	nM	4.76
87	4ih6	P26663	Kd	18000	nM	4.74
88	4j7d	P56273	Kd	20000	nM	4.7
89	2uy4	P29029	Ki	21000	nM	4.68
90	4p58	P22734	Ki	25000	nM	4.6
91	3vhk	P35968	Ki	25000	nM	4.6
92	2whp	P21836	Kd	100000	nM	4
93	5fou	O74036	Kd	113000	nM	3.95

94	4yk0	Q92793	Kd	181000	nM	3.74
95	6gjr	P62937	Kd	184000	nM	3.74
96	3isj	P0A5R0	Kd	210000	nM	3.68
97	4b3b	O74036	Kd	250000	nM	3.6
98	1pzp	P62593	Ki	490000	nM	3.31
99	5fov	O74036	Kd	1590000	nM	2.8

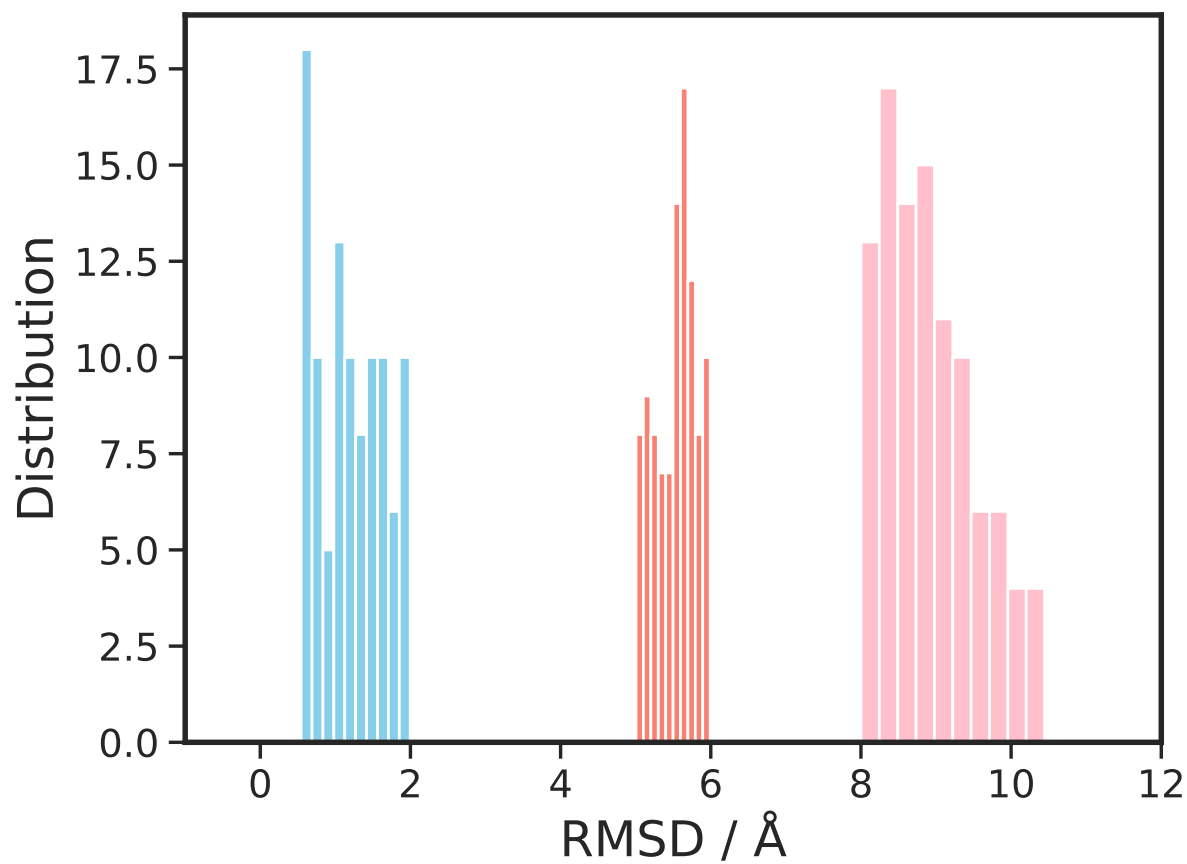


Figure S1: The distribution of RMSD for selected conformations close to 2 Å, 5 Å and 10 Å reference to the corresponding native structures.

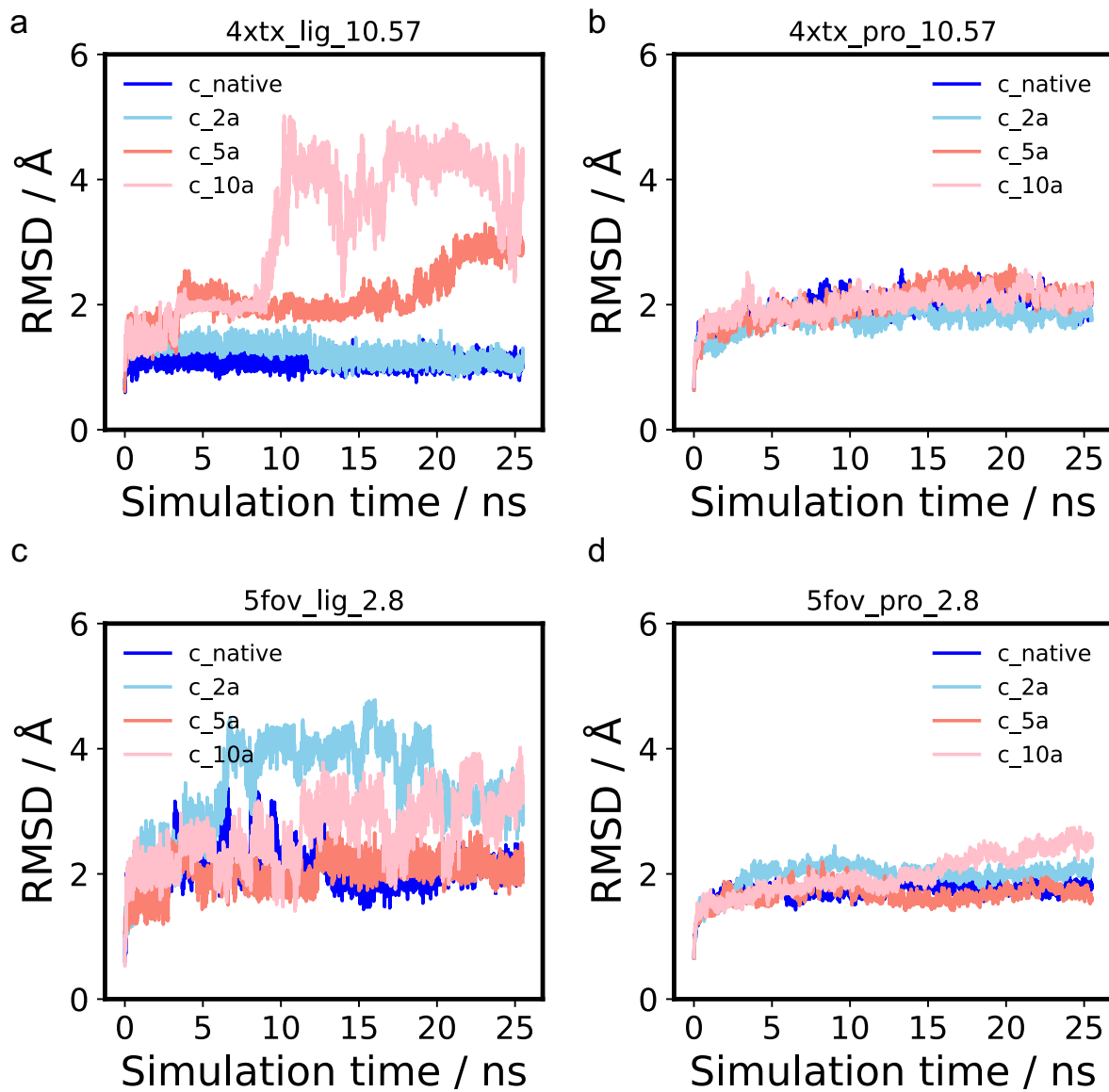


Figure S2: RMSD profile of ligand and protein of pdbid 4xtx complex and pdbid 5fov complex.

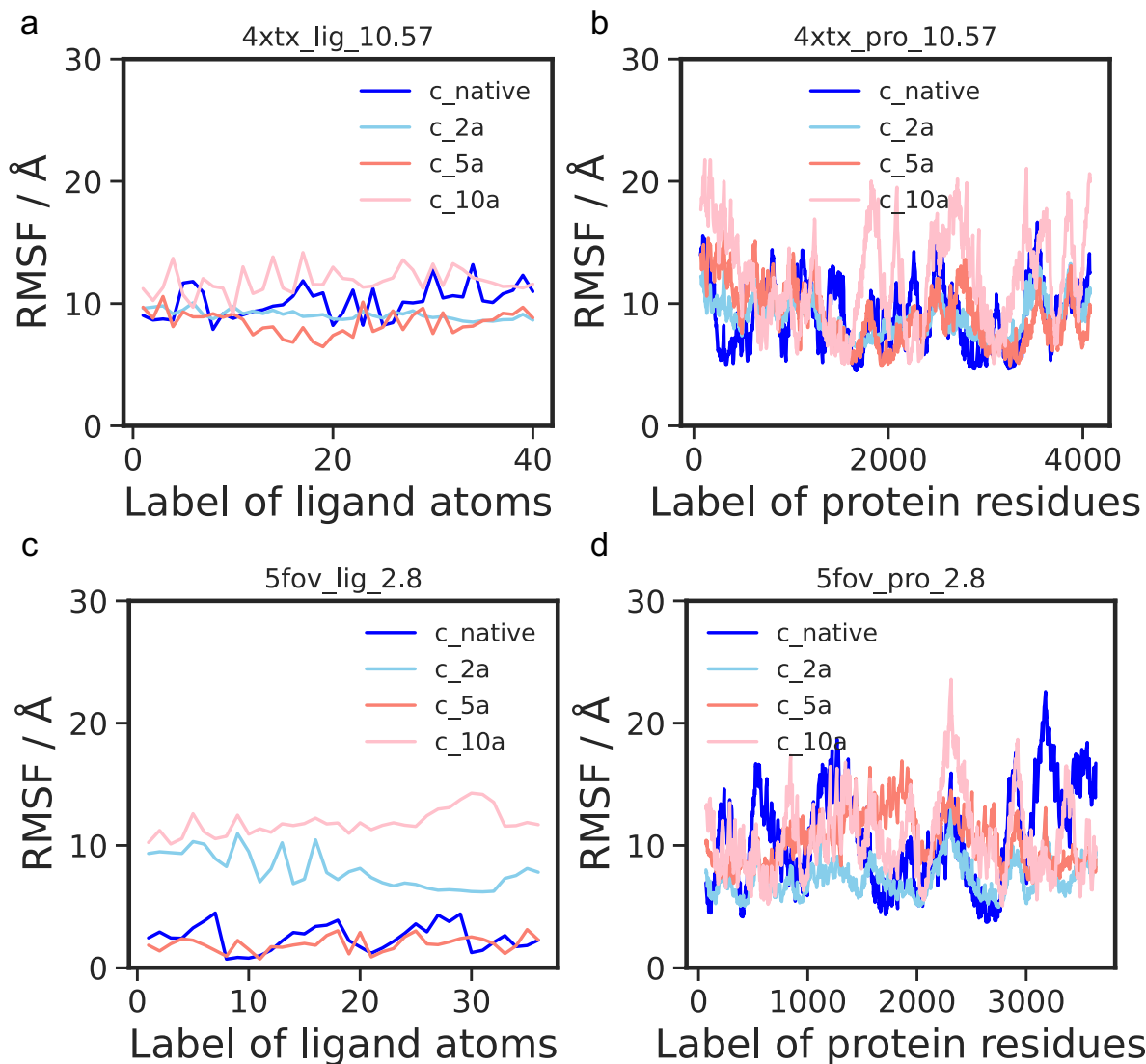


Figure S3: RMSF profile of ligand and protein of pdbid 4xtx complex and pdbid 5fov complex.

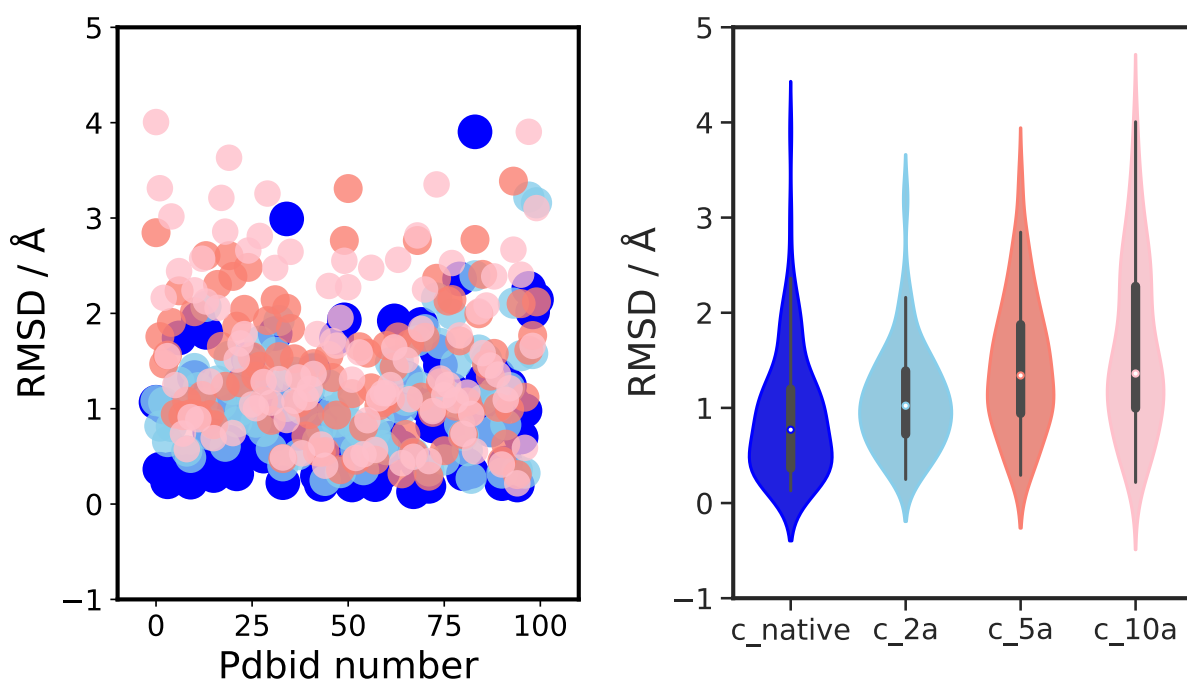


Figure S4: The distribution and boxplot of averaged RMSD of last 5 ns for selected 100 complexes.

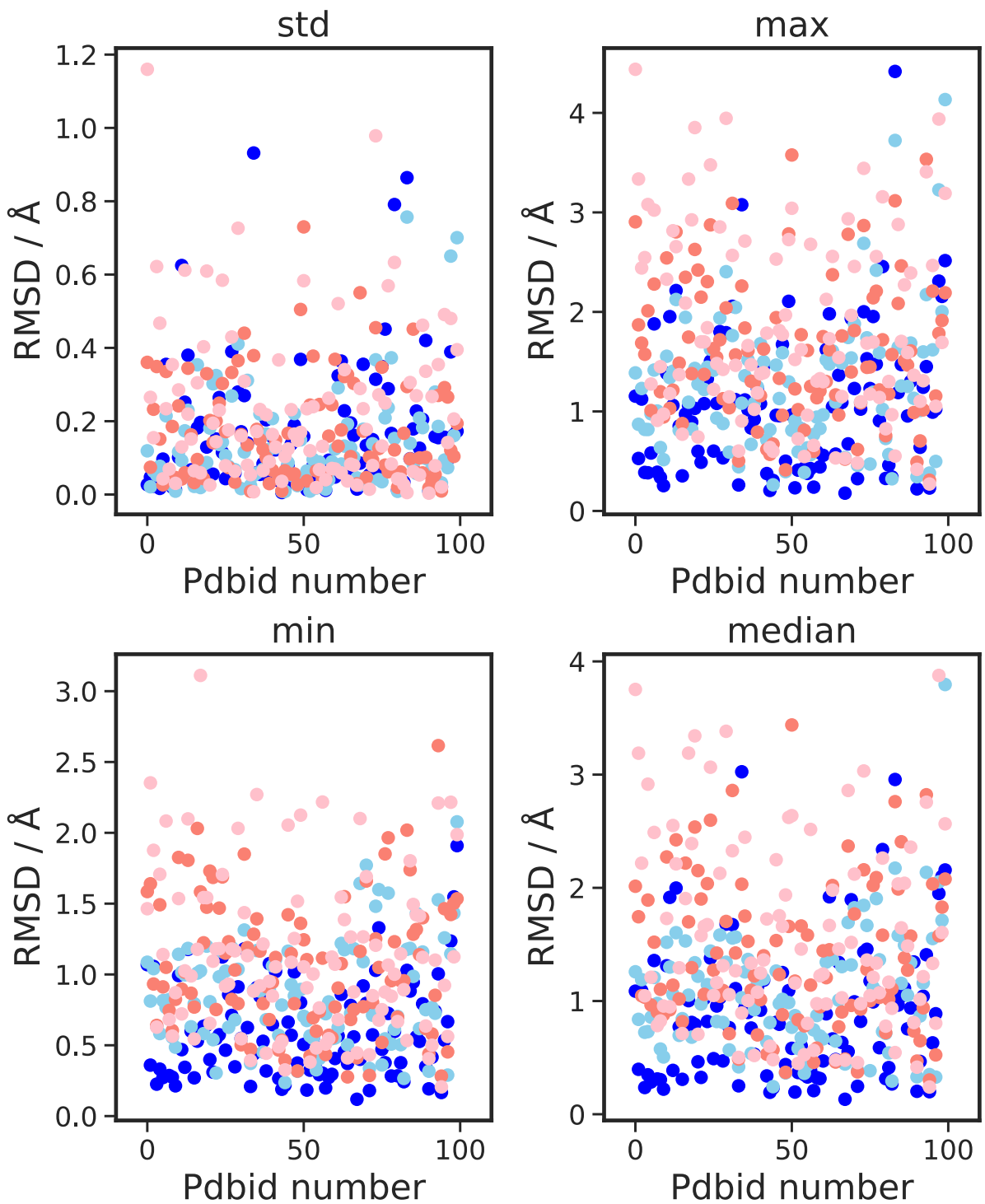


Figure S5: The distribution of the stand deviation, max, min, median values of averaged RMSD of last 5 ns for selected 100 complexes.

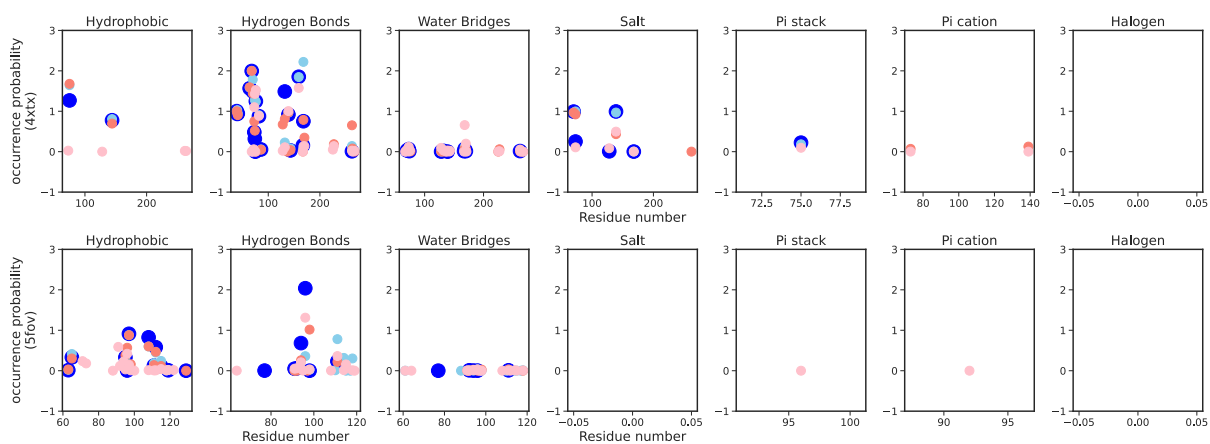


Figure S6: The occurrence frequency of each interaction pairs among seven interaction patterns detected by PLIP for the complex of pdbid 4xtx complex and pdbid 5fov complex during MD simulations of 25 ns.

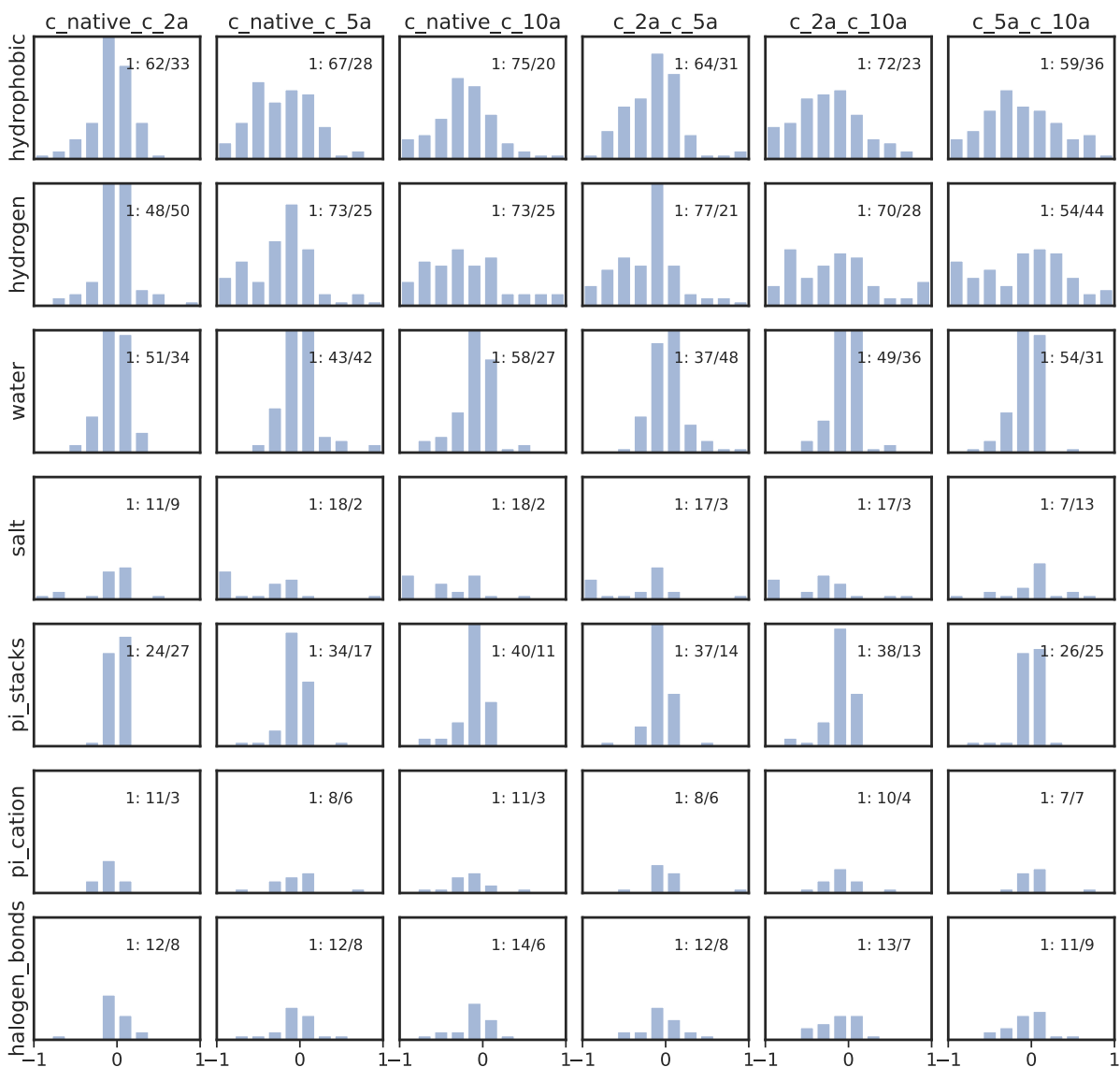


Figure S7: Difference of the highest occurrence probability for pairwise comparisons in four poses. From top to bottom, hydrophobic interaction, hydrogen bonds, water bridges, salt bridges, pi_stacking, pi_cation and halogen bonds.

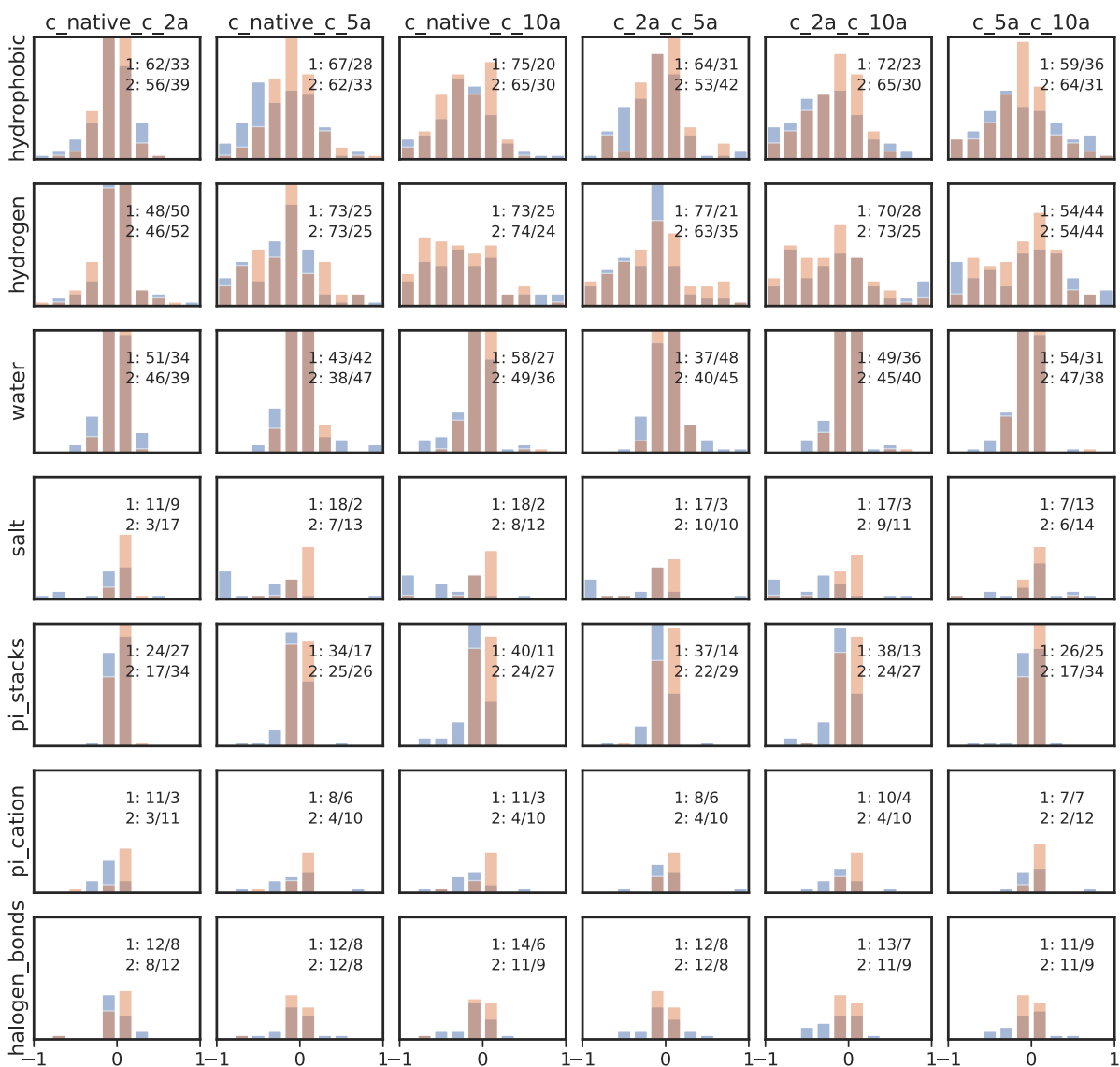


Figure S8: Difference of the top two highest occurrence probability for pairwise comparisons in four poses. From top to bottom, hydrophobic interaction, hydrogen bonds, water bridges, salt bridges, pi_stacking, pi_cation and halogen bonds.

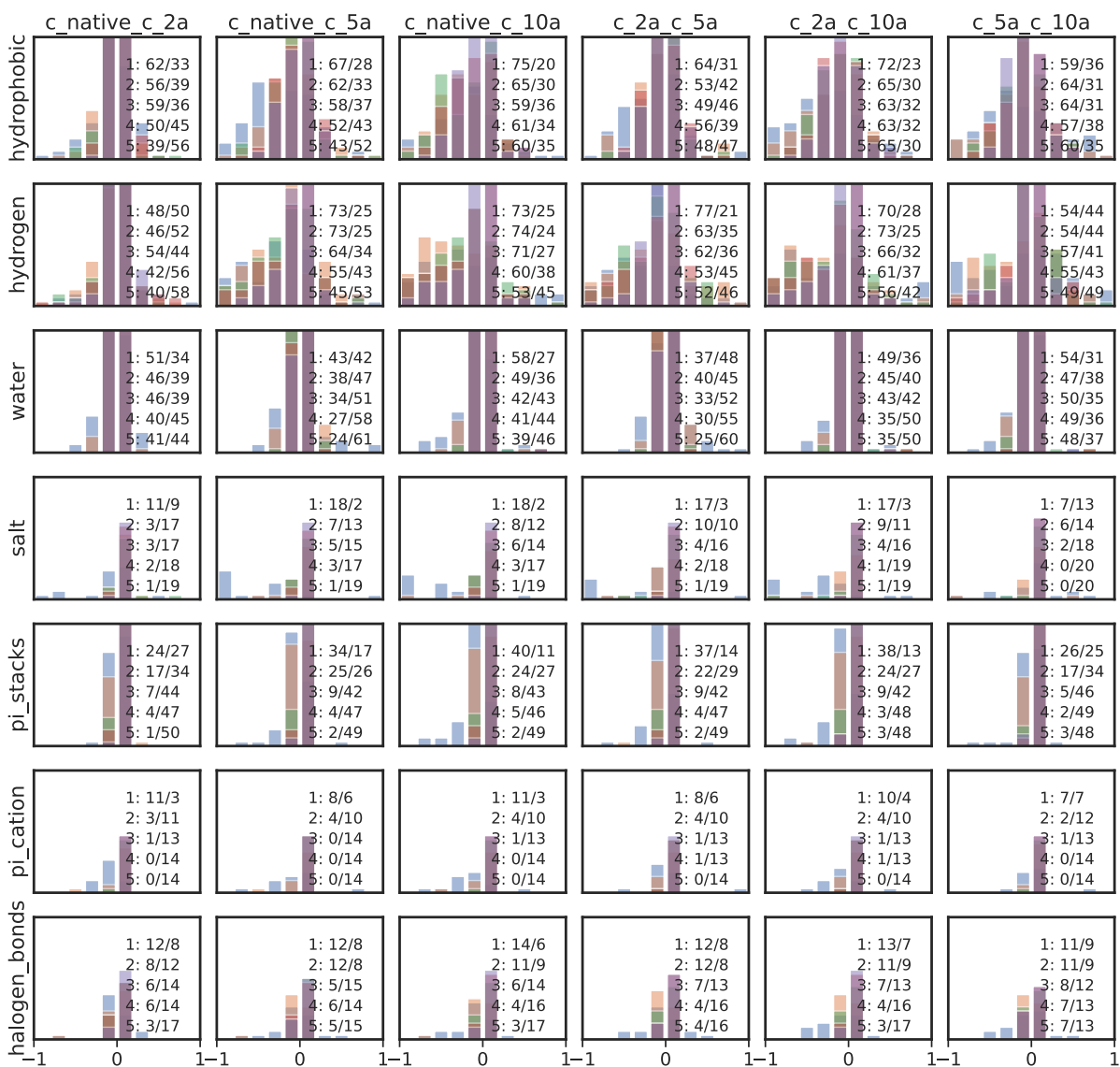


Figure S9: Difference of the top five highest occurrence probability for pairwise comparisons in four poses. From top to bottom, hydrophobic interaction, hydrogen bonds, water bridges, salt bridges, pi_stacking, pi_cation and halogen bonds.